Desalination and Water Treatment
www.deswater.com

doi: 10.1080/19443994.2015.1086696

57 (2016) 17206–17219
August

Taylor & Francis
Taylor & Francis Group

Artificial neural network (ANN) technique for modeling the mercury adsorption from aqueous solution using *Sargassum Bevanom* algae

H. Esfandian[a], M. Parvini[a,*], B. Khoshandam[a,*], A. Samadi-Maybodi[b]

[a]*Faculty of Chemical, Oil and Gas Engineering, Semnan University, Semnan, Iran, Tel. +98 231 3366929; emails: Hossein.Esfandian@gmail.com (H. Esfandian), m.parvini@sun.semnan.ac.ir (M. Parvini), bkhoshandam@semnan.ac.ir (B. Khoshandam)*

[b]*Faculty of Chemistry, Analytical Division, University of Mazandaran, Babolsar, Iran, Tel./Fax: +98 1135302350; email: samadi@umz.ac.ir*

Received 1 March 2015; Accepted 12 August 2015

ABSTRACT

In this study, the removal of mercury (Hg(II)) ions from aqueous solutions was carried out using the brown algae *Sargassum bevanom* (*S. bevanom*) as a low-cost adsorbent. The sorption of Hg(II) was facilitated through the batch method. The following are the optimum conditions of sorption: a sorbent amount of 0.4 g in 100 mL of Hg(II) solution (50 mg L^{-1}), contact time of 90 min, pH and temperature 7 and 20°C. In order to study the kinetics of removal process, three equations were employed, namely Morris–Weber, Lagergren, and pseudo-second-order. To estimate sorption capacity, the sorption data were imported in the Langmuir, Freundlich, Dubinin–Radushkevich (D–R) and Temkin models. Also, an evaluation of thermodynamic parameters, namely ΔH, ΔS, and ΔG was done subsequently. These parameters explain that the Hg(II) sorption onto the *S. bevanom* is feasible, spontaneous, and exothermic under the aforementioned conditions. The data prediction phase related to the Hg(II) sorption onto the *S. bevanom* was conducted using the artificial neural networks (ANN). A comparison was made between the Hg(II) sorption data through the ANN model. The experimental results suggested that the ANN model has a high potential for predicting the Hg(II) sorption onto *S. bevanom*.

Keywords: Mercury; Alga; Adsorption; Thermodynamic; Kinetic; ANN

1. Introduction

In the past decade, pollution of natural waters due to heavy metals led to many problems. Environmental contamination caused by heavy metals is considered a serious and widespread health problem due to their high toxicity rate and non-biodegradability as sources of pollution presently originating from growing industrial activities [1,2]. An example of an important heavy metal is mercury that has special features such as evaporation from soil and water, conversion from organic to inorganic forms by bacteria that is piled in the organisms body [3]. Mercury and its related compounds are cumulative toxins and also hazardous to human health in small quantities [4]. Mercury is toxic and non-biodegradable. Its toxicity depends on the level of exposure that can include effects such as shortness of breath in humans, panic disorder, depression, nausea, and vomiting [5,6]. Therefore, it is highly

*Corresponding authors.

important to remove heavy metals from water and wastewater. Frequency methods such as biodegradable [7], nanocomposites [8], ion exchange [9], reverse osmosis [10], solvent extraction [10], and evaporation [10] were employed for the removal of these ions.

Each of these methods has its pros and cons. Among all, the adsorption process is of highest interest due to its convenience, high efficiency, speed, and the availability of the various adsorbents [11–13]. Various factors such as metal concentration, type of adsorbent, amount of adsorbent, temperature, type of metal are effective on the process of adsorption by adsorbent. Also, the type of adsorbent is of particular importance [14,15]. Algae biomass, among all biological adsorbents, attracted much attention due to the savings in cost, less sensitivity to environmental factors and impurities [16]. A naturally available Lateritic soil was used in Ahmad and Qureshi [17] for the removal of Hg(II) from industrial wastewater. Meanwhile, an investigation of different parameters such as influence of initial concentration, pH, contact time, adsorbent dose, and adsorbent particle size on the removal of mercury ions was done. In another study, the possibility of using an inexpensive biomass obtained from prawn pond algae, namely *Sphaeroplea* algae, for the Hg(II) ions removal from aqueous solutions was studied through batch sorption method [18]. A sorbent called the Marine macro green algae *Halimeda gracilis* was also utilized as a sorbent for the Cr(VI) removal from aqueous solution. Further, the effect of various operating variables on the Cr(VI) sorption onto the *H. gracilis* and thermodynamic, kinetic, and equilibrium isotherm related to this sorption process were investigated [19].

There are too few studies in the literatures that have some relation to heavy metal adsorbent problems in terms of ANNs. ANN approach was investigated by Hosseini Asl et al. for modeling Cr(VI) adsorption from aqueous solution by zeolite that is prepared from raw fly ash (ZFA). The effects of various operational parameters such as adsorbent dosage, initial pH, temperature, and contact time are investigated to optimize the conditions required for maximum rate of Cr(VI) ions removal. An effective approach in modeling and simulating highly nonlinear multivariable relationships is using artificial neural network (ANNs). A comparison of the Cr(VI) removal efficiencies by ANN model and the experimental results revealed that ANN model is capable of estimating the Cr(VI) removal process behavior under various conditions [20]. Adsorption isotherms models and neural network were employed in Fagundes-Klen et al. to study the binary mixture of cadmium–zinc ions biosorption through species such as *Sargassum filipendula* [21]. The equilibrium concentrations of each ion in the fluid phase and ions adsorbed concentrations were used as input variables and output variables, respectively [21]. The modeling of Cu(II) adsoprtion from industrial leachate by pumice was also carried out using ANNs [22] .

In this research, an attractive adsorbent called *S. bevanom* is utilized for the treatment of Hg(II) from aqueous solution. The effects of various operational parameters, such as adsorbent dosage, initial pH, temperature, and contact time on the Hg(II) removal are also studied. Based on batch adsorption experiments, ANN model was used in this work to predict the Hg (II) removal efficiency of *S. bevanom* as a low-cost adsorbent. The Hg(II) ions adsorption from aqueous solution is optimized so that the optimal network structure can be determined. Finally, the results obtained from the models are compared with the experimental data. Also, advantages and further developments are discussed. To better understand the adsorption characteristics, some isotherm, kinetic, and thermodynamic models were used to evaluate the sorption process.

2. Materials and methods

2.1. Collection of biomass and mercury solution preparation

S. bevanom algae was extracted from the Persian Gulf (Bandar Boshehr, Iran). The collected biomass was washed with distilled water to remove silt, sand, and other epiphytic organisms. After cleaning, the algae was dried and stored at room temperature. Then, the acid treated *S. bevanom* was prepared by mixing the *S. bevanom* in a 0.1 M HCl solution and stirring the mixture at 200 rpm for 8 h at room temperature. Then, the alga was centrifuged, washed with the physiological saline solution and dried in an oven at 60 °C. Later, it was ground on an agate stone pestle mortar and sieved to select the particles between 200 and 300 mesh sizes to be used in the sorption process [23–26]. Mercury solutions were prepared according to the standard methods [27].

2.2. Instrumentation

In this research, the description of *S. bevanom* surface was carried out with a very high level of magnification by means of the scanning electron microscopy (SEM) (HITACHI) Model S-4160). The *S. bevanom* was covered with gold and palladium to increase the conductivity.

To determine the mercury concentration in the aqueous solution, Flame Atomic Absorption Spectrophotometer (Model 929, Unicam) was used.

2.3. Batch adsorption experiments

In this study, the adsorption experiments were performed to study the effect of the experimental conditions on the achievement of maximum rate of mercury removal. Different parameters, such as the effects of pH, contact time, initial concentration of Hg(II), and the dosage of the adsorbent, were considered to optimize the Hg(II) removal process. In this part of the study, isotherm and kinetic evaluations were carried out. The adsorption tests were performed in magnetic mixer. The magnetic mixer worked at 300 rpm throughout the study with 100 mL Hg(II) solution which was prepared by diluting 1 g/L stock solution. At the end of the pre-determined time intervals, the sorbate was filtered and the concentration of Hg(II) was determined. All experiments were done twice and the adsorbed concentrations given led to the duplicate experimental results. In all experiments, powder was the form of *S. Bevanom*. The Hg(II) efficiency based on percent removal was calculated as follows:

$$\%\,\text{Removal} = \frac{C_\text{i} - C_\text{f}}{C_\text{i}} \times 100 \tag{1}$$

where C_i is the initial concentration (mg L^{-1}); C_f is the final concentration (mg L^{-1}); q is the amount of metal adsorbed per the specific amount of adsorbent (mg g^{-1}). The sorption capacity at time t, q_t (mg g^{-1}), was given by:

$$q_t = \frac{(C_\text{i} - C_t)V}{m} \tag{2}$$

where C_i and C_t (mg L^{-1}) are liquid-phase concentrations of solutes at initial and a given time t, respectively; V is the solution volume; m is the mass of *S. Bevanom* (g). The amount of adsorption at equilibrium, q_e was obtained by:

$$q_\text{e} = \frac{(C_\text{i} - C_\text{e})V}{m} \tag{3}$$

where C_e (mg L^{-1}) is the ion concentration at equilibrium.

2.4. ANN modeling

The development of the empirical models by way of numerical estimation techniques such as the ANN can be regarded as powerful alternatives for the prediction of adsorption system. ANNs were previously developed from the basic concept of AI that tried to simulate the human brain and nervous system processes [28,29]. They contain a series of mathematical correlation that are being used to simulate the learning and memorizing operations. ANNs learn through examples in which an actual measured set of input variables and corresponding output are presented to determine the rules that control the relationships between the variables [26]. ANNs are considered a powerful means for capturing non linear effects and are practically applicable to any situation with a highly nonlinear relationship between the dependent and independent variables [30]. Networks are made up of three main layers, namely input, hidden, and output layers [31,32]. In this research, a multi-layer feed-forward neural network was used. In this set of networks, information moves forward in merely one direction from the input layer toward the hidden layer and finally to the output. Running of neural network is normally carried out in two stages, namely learning or training and testing. The network architecture is represented by l, m, n, where l neurons are present at input layer (equal to the number of inputs in the network), m neurons at the hidden layer (optimized through experimentation), and n neurons at the output layer in terms of the number of desired outputs [29]. All experimental data are classified into three sets, namely training (70%), validation (15%) and testing (15%). The complete data are normalized in (0–1). Therefore, data (X_i) are converted into a normalized value (Xnormal) as shown in the following [28,29]:

$$X_\text{normal} = \frac{(X_i - X_\text{min})}{(X_\text{max} - X_\text{min})} \tag{4}$$

X_min and X_max are minimum and maximum actual experimental data, respectively. The input signals are adjusted by the interconnection weight, aka weight factor (W_{ij}). It represents the interconnection of ith node of the first layer with the jth node of the second layer. Then, the sum of modified signals (total activation) is modified by a sigmoid transfer function and the output is collected at output layer [29,32].

The ANN model training will be more efficient provided preprocessing steps are performed on the input and target data [33]. To evaluate the integrity of the fit of experimental data and the employed models prediction accuracy, the following Eq. (5) is utilized:

$$\text{MSE} = \frac{\sum \left| (q_\text{exp} - q_\text{cal})/q_\text{exp} \right| \times 100}{N} \tag{5}$$

To find the optimum number of neurons at hidden layer, the network is tested with different number of neurons through the observation of the mean squared error (MSE). The network is tested with different number of neurons to find their optimum number at the hidden layer through the observation of the MSE. The lowest mean square error is given for six neurons. Also, the maximum R^2 is obtained for six neurons. Results obtained from the prediction carried out by neural network for training, validation, and testing are shown in Table 1.

3. Results and discussion

3.1. Characterization of the biosorbent

The chemical and physical properties of the raw and acid-treated *S. bevanom* were determined by the standard methods [23–25]. The surface area for both biomasses which was determined by Quantasorb surface area analyzer equaled 1.24 $m^2\ g^{-1}$. The elemental analysis showed the biosorbents composition as $C = 22.4\%$; $N = 4.18\%$; $S = 1.64\%$. The calculated humidity and the zeta potential were 1.35, 3.31% and −0.058, −0.076 V for the raw and acid-treated *S. bevanom*, respectively. The obtained density of the biosorbent was 1.1 $g\ cm^{-3}$.

The surface structures related to the original acid-treated *S. bevanom* particles which were imaged with different magnifications are presented in Fig. 1(a)–(c). As shown in Fig. 1(a) and (b), the original adsorbent was nonporous. Fig. 1(c) shows *S. bevanom* after being treated by acid. As can be seen, the *S. bevanom* surface is changed and the porosity of adsorbent is increased [23,24].

Table 1
Results of neural network for prediction of adsorption amount

		Sample	Regression (R^2)
4 neuron	Train	26	0.967
	Validation	6	0.965
	Testing	6	0.931
5 neuron	Train	26	0.918
	Validation	6	0.923
	Testing	6	0.955
6 neuron	Train	26	0.987
	Validation	6	0.994
	Testing	6	0.996
7 neuron	Train	26	0.965
	Validation	6	0.961
	Testing	6	0.958

3.2. Effect of pH on Hg(II) sorption

Results of the earlier studies conducted on heavy metal biosorption revealed that adsorption depends on the solution pH because it affects biosorbent surface charge, degree of ionization, and the species of biosorbent [34]. Thus, the effect of solutions pH (H^+ ion concentration) on the adsorption percentage of mercury ions was studied at different pH in the range of 1–10 (Fig. 2). Less mercury uptake at low pH values is indicative of protons competition for the same binding sites on the algal cell wall. Additionally, it was found out that the Hg(II) uptake increases with every increase in pH and reaches a maximum value at pH 7.0. As the aqueous solution pH increases, the negative charge density of the adsorbent increases accordingly. Therefore, the Hg(II) ions uptake with an increasing pH is due to an increasing negative charge density on the adsorbent surface and it is also responsible for a drop in the Hg(II) sorption at a low hydrogen ion concentration. Hence, for subsequent studies, an optimum pH 7 is chosen. The agreement between the ANN model predictions and the experimental data, as a function of initial pH, is shown in Fig. 2. It can be seen from this plot that results obtained from the proposed ANN model are in good agreement with the experimental data.

3.3. Effect of contact time

Fig. 3 shows the effect of contact time on the Hg(II) sorption by *S. Bevanom*. In these cases, the initial Hg (II) concentration was 50 $mg\ L^{-1}$. Also, a pH 7 was used for Hg(II). Moreover, algae dose of 0.4 g in 100 mL were utilized. For Hg(II), the sorption rate goes up to 90.24 when contact time is 90 min and then little change of sorption rate is seen. Subsequently, the initial rapid adsorption yields to a very slow approach to equilibrium and saturation is reached in 90 min. For further optimization of other parameters, the contact time 90 min was taken as the equilibrium time corresponding to adsorbate and adsorbent. Later, the experimental data and ANN calculated outputs were compared. The results suggested that the ANN model shows a good performance during the prediction of the experimental data.

3.4. Kinetics of sorption

Most of the adsorption transformation processes of various solid phases are time dependent. Knowledge of the kinetics of these processes is important in understanding the dynamic interactions of mercury with algae and also to predicting their fate with

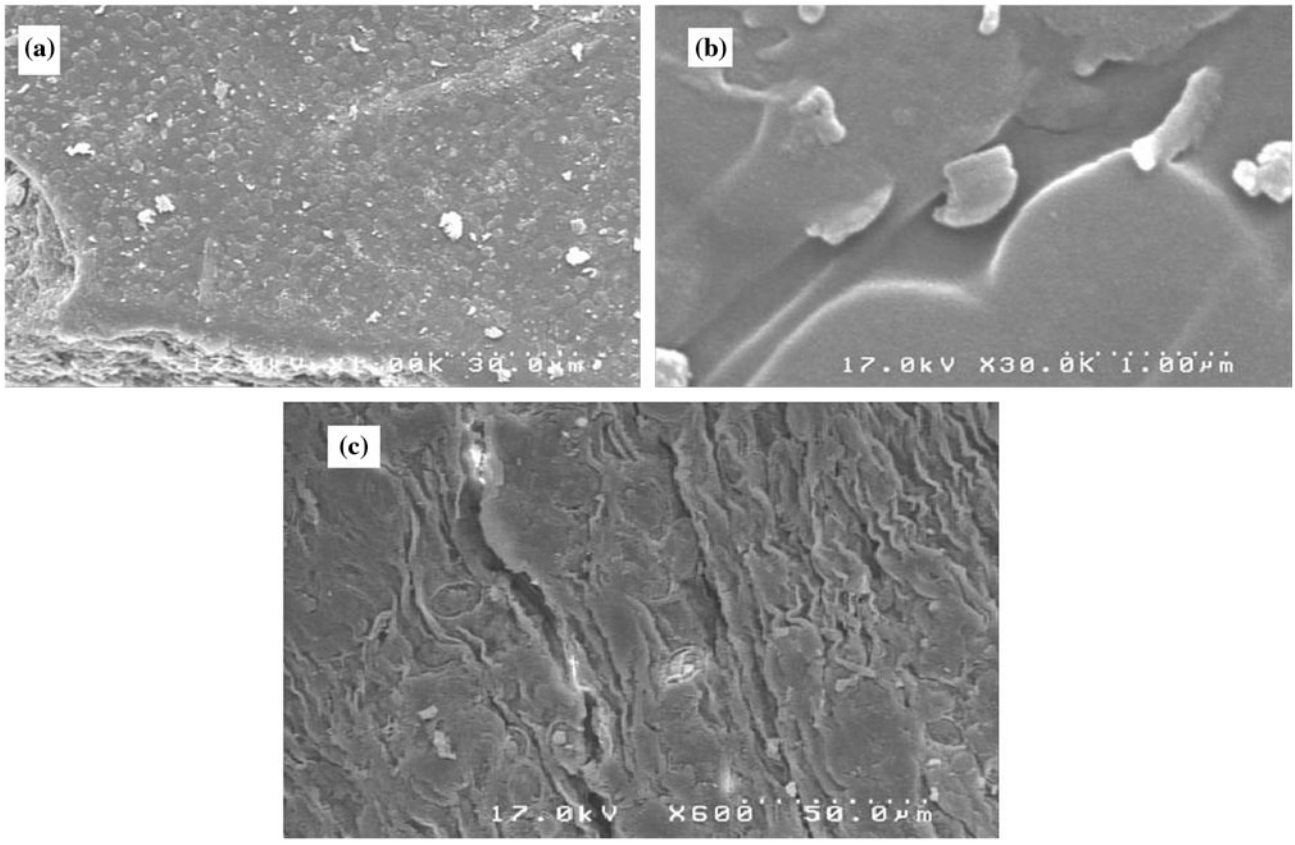

Fig. 1. (a) Field emission scanning electron microscope (FE-SEM) image of *S. bevanom*. FE-SEM image of *S. bevanom*, (b) with more significance and (c) after having been acid treated by HCl.

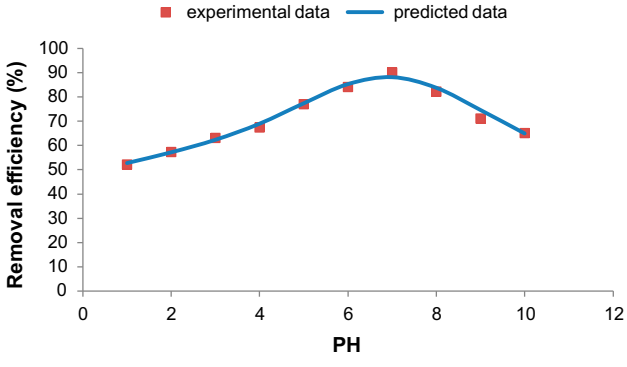

Fig. 2. The effect of pH on the removal efficiency and comparison between experimental and predicted data (the initial concentration, contact time, volume of solution, and amount of adsorbent were 50 mg L^{-1}, 90 min, 100 mL, and 0.4 g, respectively).

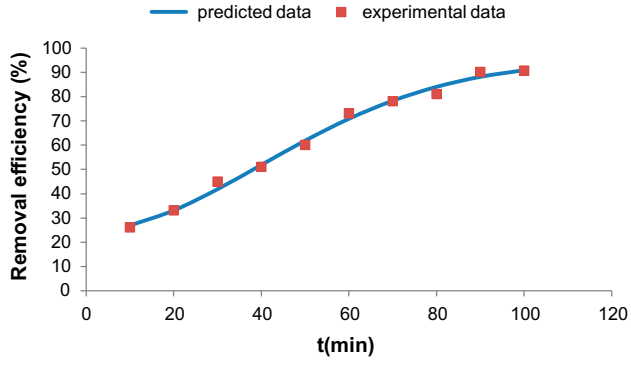

Fig. 3. The effect of contact time on the removal efficiency and comparison between experimental and predicted data (the initial concentration, pH, volume of solution, and amount of adsorbent were 50 mg L^{-1}, 7, 100 mL, and 0.4 g, respectively).

time [35]. Different kinetic models, namely Morris–Weber, Lagergren, and pseudo-second-order models were used because of their validity with the experimental adsorption data for the Hg(II) onto *S. Bevanom*. It was said to offer no mass transfer (both external and internal external) resistance to the overall adsorption process. Therefore, the kinetic can be examined by the residual metal ion concentration in the solution.

The study of adsorption kinetics explains the solute uptake rate. Clearly, this rate controls the residence time of adsorbate uptake at the solid–solution interface including the diffusion process.

The kinetic data of Hg(II) ions sorption onto algae were subjected to Morris–Weber Eq. (6) to explain the change in the concentration of sorbate onto sorbent with shaking time [36]:

$$q_t = K_{id}(t)^{0.5} + C \quad (6)$$

where q_t is the Hg(II) ions sorbed concentration at time "t". The plot related to q_t vs. $t^{0.5}$ is shown in Fig. 4. The rate constant value of the Morris–Weber transport, K_{id}, is calculated using the slope of the linear plot that is given in Fig. 4. The rate constant $K_{id} = 0.0007\ \text{min}^{-1}$ was calculated using the slope of the straight line with a correlation factor of 0.9833.

Internal particle diffusion might involve pore and/or surface diffusion. The intraparticle diffusion plots show multi-linearity in the process suggesting that there are three operational steps. The first step refers to the diffusion of adsorbate through the solution to the external surface of the adsorbent or the boundary surface diffusion of the sorbate molecules. The second step explains the gradual sorption where intraparticle diffusion is rate limiting. Finally, the third step is related to the final equilibrium because of the extremely low sorbate concentration remaining in the solution and the reduction of interior active sites. The three steps in the plot indicate that the sorption process occurs by surface adsorption and intraparticle diffusion.

In 1898, a pseudo-first-order equation was suggested by Lagergren [37] for the sorption of liquid/solid system in terms of solid capacity. It supposes that the sorbate uptake rate of change with time is directly relevant to the difference in the saturation concentration and the amount of solid uptake with time. The Lagergren equation is the most widely accepted rate equation in liquid phase sorption. The general equation is given as:

$$\log(q_e - q_t) = \log q_e - \left(\frac{K}{2.303}\right)t \quad (7)$$

where q_e is the sorbed concentration at equilibrium and K is the first-order rate constant. The linear plot related to $\log(q_e - q_t)$ against time "t" (Fig. 5) indicates the applicability of the above equation for Hg(II) ions sorption onto algae. The rate constant, $K = 0.0463\ \text{min}^{-1}$, was calculated using the slope of the straight line with a correlation factor 0.7404. The results of kinetics are:

The Hg(II) ions sorption onto algae following a pseudo-second-order kinetics can be explained as Eq. (8):

$$\frac{t}{q_t} = \frac{1}{Kq_e^2} + \frac{t}{q_e} \quad (8)$$

where q_t and q_e are the amount of ion adsorbed at time t and at equilibrium (mg g^{-1}); k_2 (g mg^{-1} min^{-1}) is the pseudo-second-order rate constant for the adsorption process. One can linearize this equation to four different forms. The different linearized types of the pseudo-second-order equation are presented in Table 2. From the results, the mercury adsorption by algae can be adjusted using Type 1, Type 2, Type 3, and Type 4 equations. Also, Type 2 equation offers the best correlation factor. Figs. 6–9 shows the linear plots of pseudo-second-order equations.

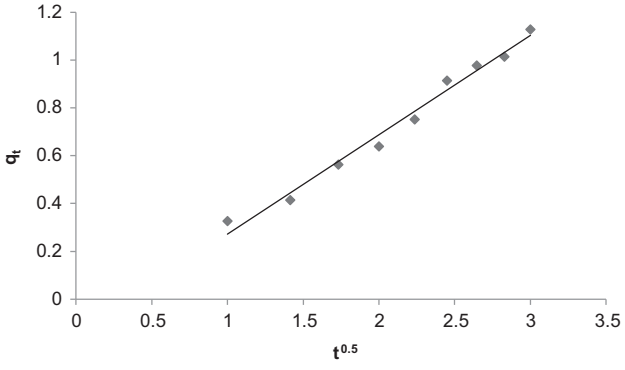

Fig. 4. Morris–Weber plot of mercury ions sorption onto *S. bevanom* (the initial concentration, pH, volume of solution and amount of adsorbent were 50 mg L^{-1}, 7, 100 mL, and 0.4 g, respectively).

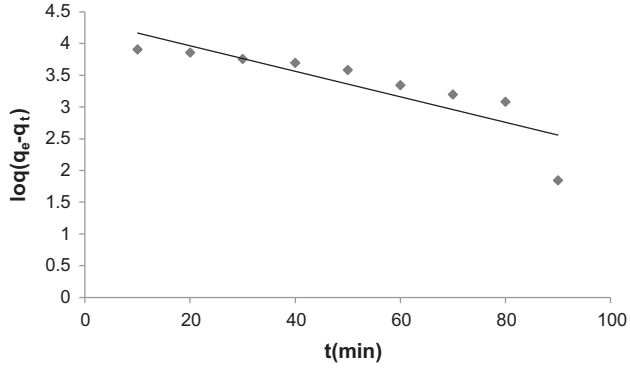

Fig. 5. Validation of Lagergren plot of mercury ions sorption onto *S. bevanom* (the initial concentration, pH, volume of solution, and amount of ad sorbent were 50 mg L^{-1}, 7, 100 mL, and 0 .4 g, respectively).

Table 2
Kinetic constants for mercury adsorption

	K_{id} (min^{-1})	R^2	
Morris–Weber equation	0.0007	0.9833	
Pseudo-first-order kinetic model	K (min^{-1})	q_e (mg g^{-1})	R^2
	0.0463	23302.36	0.7404
Pseudo-second-order kinetic model	k_2 (g mg^{-1} min^{-1})	q_e (mg g^{-1})	R^2
Type 1 $\frac{t}{q_t} = \frac{1}{k_2 q_e^2} + \frac{1}{q_e} t$ $\frac{t}{q_t}$ vs. t	7.14×10^{-7}	20,000	0.9295
Type 2 $\frac{1}{q_t} = \frac{1}{q_e} + \left(\frac{1}{k_2 q_e^2}\right)\frac{1}{t}$ $\frac{1}{q_t}$ vs. $\frac{1}{t}$	2.56×10^{-6}	12,500	0.9305
Type 3 $q_t = q_e - \left(\frac{1}{k_2 q_e}\right)\frac{q_t}{t}$ q_t vs. $\frac{q_t}{t}$	1.7×10^{-6}	14,644	0.7361
Type 4 $\frac{q_t}{t} = k_2 q_e^2 - k_2 q_e (q_t)$ $\frac{q_t}{t}$ vs. q_t	1.0699×10^{-6}	17,103.8	0.7361

The kinetic data suggested that the adsorption process was controlled by the pseudo-second-order equation. Also, this indicates the assumption behind the pseudo-second-order model that the mercury ions uptake process originates from chemisorptions. The assumption behind the pseudo-second-order kinetic model is that the rate-limiting step might be involvement of valence forces by chemisorption through sharing or exchanging electrons between adsorbent and adsorbate. It should be mentioned that the adsorption of multi-metal ions by an adsorbent has a complicated mechanism. The behavior of each metal ion in a multi-metal ions system strongly depends on the concentration and the properties of other present ions, pH of the solution, physical and chemical properties of both the adsorbent and adsorbate. The shape and coefficients of the adsorption kinetics of the system were influenced by both the interaction and competition effects among the multi-metal ions [38].

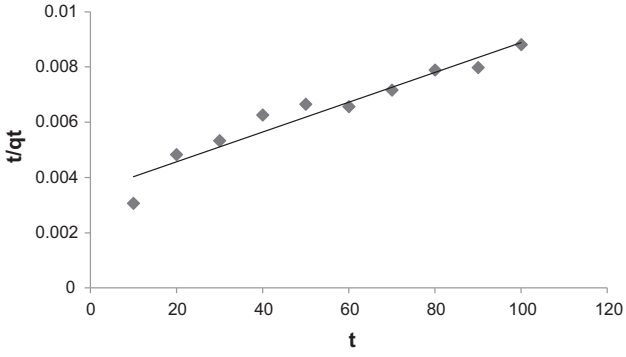

Fig. 6. Pseudo-second-order (Type 1) plot of mercury ions sorption onto *S. bevanom* (the initial concentration, pH, volume of solution, and amount of adsorbent were 50 mg L^{-1}, 7, 100 mL, and 0.4 g, respectively).

3.5. Effect of adsorbent dosage

To evaluate the effect of biosorbent dose, it was studied at a dose between 0.1 and 0.45 g in a 100 mL aqueous solution. The experiments were performed at 20°C temperature with an optimum pH. The initial mercury ion concentration was 50 mg L^{-1}. It was later found out that the percentage of Hg(II) adsorption onto *S. bevanom* increased rapidly with the increase in the adsorbent concentration (Fig. 10). This is an expected result because the increase in the adsorbent dose leads to greater surface area. At higher concentrations, the Hg(II) equilibrium uptake did not increase greatly with the increase in *S. bevanom*. For further studies, a dose of 0.4 g acid-treated *S. bevanom*

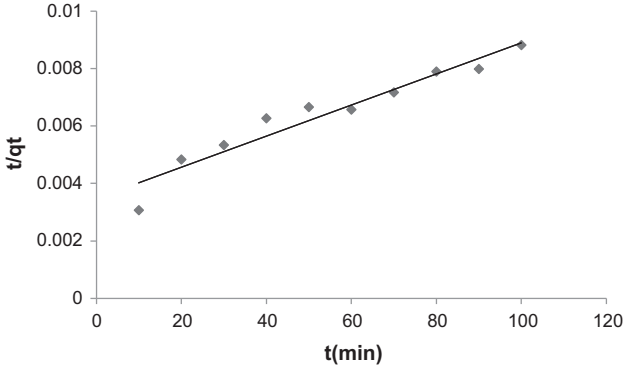

Fig. 7. Pseudo-second-order (Type 2) plot of mercury ions sorption onto *S. bevanom* (the initial concentration, pH, volume of solution, and amount of adsorbent were 50 mg L^{-1}, 7, 100 mL, and 0.4 g, respectively).

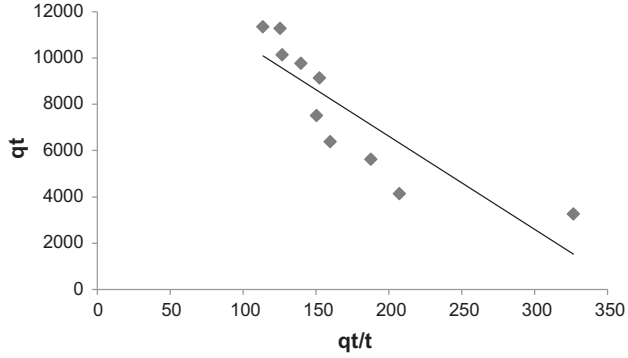

Fig. 8. Pseudo-second-order (Type 3) plot of mercury ions sorption onto *S. bevanom* (the initial concentration, pH, volume of solution, and amount of adsorbent were 50 mg L^{-1}, 7, 100 mL, and 0.4 g, respectively).

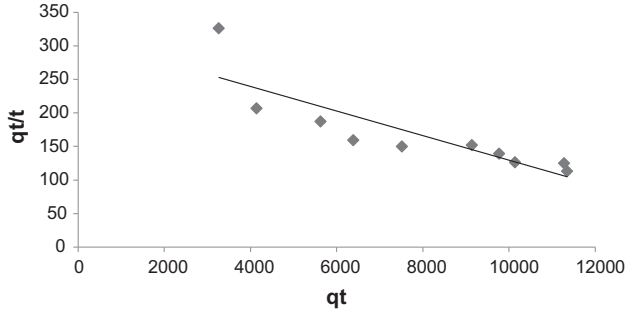

Fig. 9. Pseudo-second-order (Type 4) plot of mercury ions sorption onto *S. bevanom* (the initial concentration, pH, volume of solution, and amount of adsorbent were 50 mg L^{-1}, 7, 100 mL, and 0.4 g, respectively).

in a 100 mL aqueous solution was selected. The experimental data and the ANN outputs, as a function of biomass dosages (Fig. 10), showed that the model performance is in good agreement with the experimental data.

3.6. Effect of initial concentration of mercury on the adsorption

The batch-mode experiments were carried out at ambient temperature (20°C) to study the effect of initial Hg(II) concentration on Hg(II) adsorption onto *S. Bevanom*. The Hg(II) solution initial concentration was ranging from 50 to 210 mg L^{-1} with an optimum adsorbent dose, contact time, and pH (Fig. 11). It is clear from the result that the Hg(II) percentage removal dropped from 90.14 to 62.66% for an initial Hg(II) concentration of 50–210 mg L^{-1}. The results suggest that there is a reduction in Hg(II) adsorption due to the lack of available active sites required for

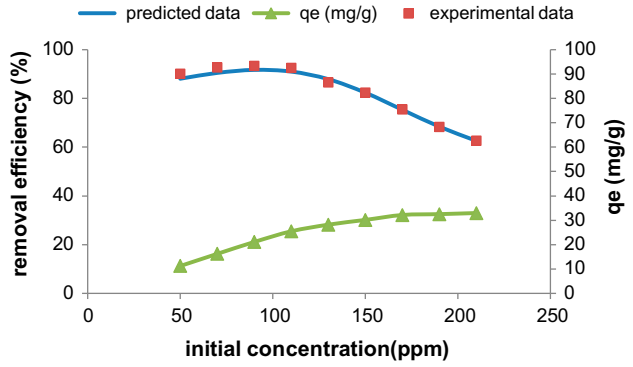

Fig. 10. The effect of initial concentration on the adsorption capacity (pH, volume of solution, contact time and amount of adsorbent were 7, 100 mL, 90 min, and 0.4 respectively).

the high initial concentration of Hg(II). The Hg(II) higher uptake at low concentration might be related to the accessibility of more active sites on the surface of the adsorbent for lesser number of adsorbate species. An investigation of the experimental data and ANN outputs, as a function of initial Hg(II) concentration (Fig. 11), showed that the performance of the model is in good agreement with the experimental data.

The Fig. 11 data were fitted to Langmuir, Freundlich, Temkin, and Dubinin–Radushkevich (D–R) models to examine the models constants adsorption isotherms.

3.7. The isotherm model

The adsorption isotherm is based on the supposition that every adsorption site is equivalent and independent of the accessibility or inaccessibility of

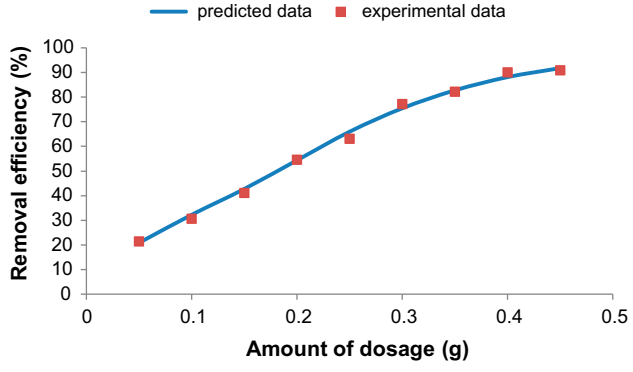

Fig. 11. The effect of amount of adsorbent on the removal efficiency and comparison between experimental and predicted data (pH, volume of solution, contact time and initial concentration were 7, 100 mL, 90 min, and 50 mg L^{-1} respectively).

Table 3
Isotherm constants for mercury adsorption

			K_L (min^{-1})	q_m (mg g^{-1})	R_L	R^2
Langmuir equation	Type 1	$\frac{C_e}{q_e} = \frac{1}{(q_m K_L)} + \left(\frac{1}{q_m}\right) C_e$ C_e/q_e vs. C_e	5.6	35.59	0.003559–0.00085	0.9937
	Type 2	$\frac{1}{q_e} = \frac{1}{(q_m K_L C_e)} + \left(\frac{1}{q_m}\right)$ $1/q_e$ vs. $1/C_e$	0.1589	37.4532	0.0023–0.000548	0.962
	Type 3	$q_e = q_m - \left(\frac{1}{K_L}\right)\frac{q_e}{C_e}$ q_e vs. q_e/C_e	0.1641	36.446	0.087336–0.022277	0.8985
	Type 4	$\frac{q_e}{C_e} = K_l q_m - K_l q_e$ q_e/C_e vs. q_e	0.1594	38.14	0.002349–0.00056	0.8331
Freundlich equation				K (min^{-1})	n	R^2
				0.0736	0.402	0.8114
Temkin equation				K_T	B	R^2
				3.104	6.4481	0.7222
D–R equation				β	q_m	R^2
				4×10^{-6}	32.632	0.9118

the adjacent sites [39]. Isotherms reveal that there is a relationship between metal concentration in solution and the amount of nitrate sorbed on a specific sorbent at a constant temperature.

3.7.1. The Langmuir isotherm model

The Langmuir isotherm model supposes that the adsorption occurs in a monolayer. Also, the absorption sites that are located on the adsorbent surface are uniform and all of them have the same absorbing ability. This isotherm model is often suggested in the form of the following equation [40]:

$$q_e = \frac{q_m K_L C_e}{1 + K_L C_e} \tag{9}$$

where q_e is the mercury adsorbed per specific amount of adsorbent, C_e is the concentration of the mercury solution (mg L^{-1}) at equilibrium, and q_m is the maximum amount of adsorption mercury ions (mg g^{-1}). One can rearrange the Langmuir equation into four various linear types presented in Table 3. The best fit was achieved by the Langmuir-Type 1 in comparison with other Langmuir models. Figs. 12–15 depict the linear plots of different types of this equation. The basic features and practicality of the Langmuir isotherm regarding a dimensionless constant separation factor or equilibrium parameter R_L are defined as the following equation [41]:

$$R_L = \frac{1}{1 + K_L C_i} \tag{10}$$

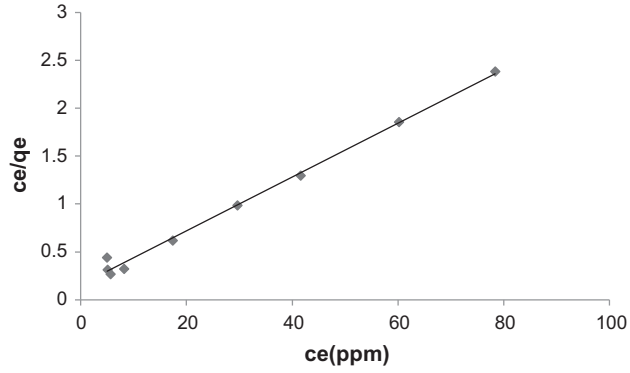

Fig. 12. Langmuir sorption isotherm (Type 1) of mercury ions onto *S. bevanom* (the initial concentration, pH, volume of solution, and contact time was 50 mg L^{-1}, 7, 100 mL, and 90 min, respectively).

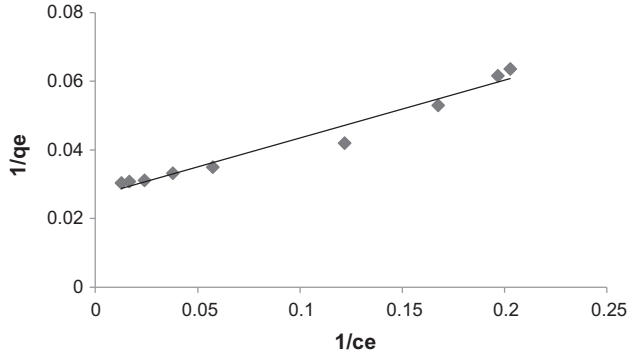

Fig. 13. Langmuir sorption isotherm (Type 2) of mercury ions onto *S. bevanom* (the initial concentration, pH, volume of solution, and contact time was 50 mg L^{-1}, 7, 100 mL, and 90 min, respectively).

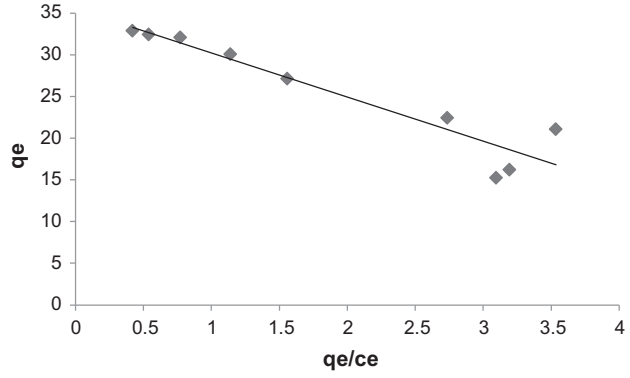

Fig. 14. Langmuir sorption isotherm (Type 3) of mercury ions onto *S. bevanom* (the initial concentration, pH, volume of solution, and contact time was 50 mg L^{-1}, 7, 100 mL, and 90 min, respectively).

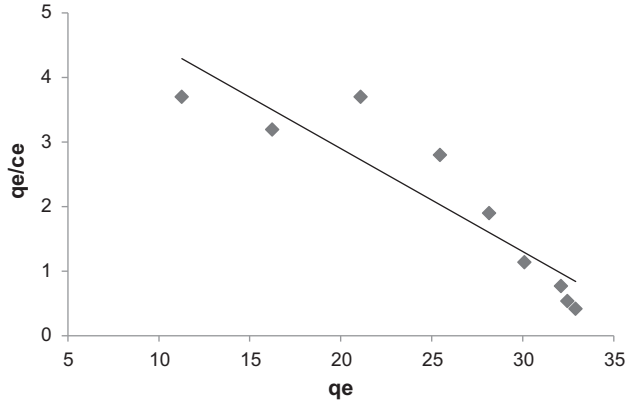

Fig. 15. Langmuir sorption isotherm (Type 4) of mercury ions onto *S. bevanom* (the initial concentration, pH, volume of solution, and contact time was 50 mg L^{-1}, 7, 100 mL, and 90 min, respectively).

where K_L is the Langmuir constant and C_i is the initial concentration of mercury. The desired value of absorption may range from 0 to 1.

3.7.2. The Freundlich isotherm model

While Langmuir isotherm supposes that the adsorption enthalpy is independent of the adsorbed amount, one can derive the empirical Freundlich equation based on the sorption on heterogeneous surface assuming a logarithmic drop in the adsorption enthalpy with an increase in the fraction of the occupied sites. The Freundlich equation is completely empirical in terms of the sorption on heterogeneous surface. It is given by the following equation [42]:

$$q_e = K_F C_e^{\frac{1}{n}} \tag{11}$$

where K_F and $(1/n)$ are the Freundlich constants related to the adsorption capacity and adsorption intensity, respectively. The equilibrium constants are evaluated from the intercept and the slope of the linear plot of $\log q_e$ vs. $\log C_e$ based on experimental data. One can linearize the Freundlich equation in logarithmic form with the purpose of determining the Freundlich constants using the following equation:

$$\log(q_e) = \log(K_F) + \frac{1}{n}\log C_e \tag{12}$$

The intercept and the slope correspond to K_F and $(1/n)$, respectively. It was discovered that the $\log q_e$ and $\log C_e$ plot yields a straight line (Fig. 16). The results are presented in Table 3.

3.7.3. The Temkin isotherm model

This isotherm model uses a factor to provide for the inclusion of interactions between the adsorbents and adsorbates. Temkin model enjoys the following conditions: (i) the adsorption heat related to all molecules that are present in the layer decreases linearly with the coverage due to the adsorbent–adsorbate interactions; (ii) to characterize the adsorption, a uniform distribution of binding energies is used up to the maximum binding energy. The Temkin isotherm suggests that the decrease in the adsorption heat is more linear rather than logarithmic as already implied by the Freundlich equation. The Temkin isotherm is normally used in the form of the following equation [24,43]:

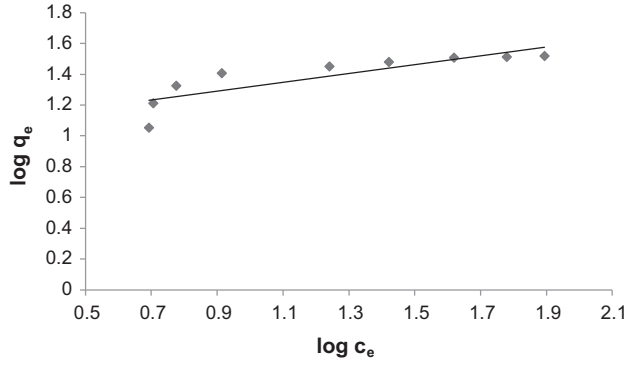

Fig. 16. Freundlich sorption isotherm of mercury ions onto *S. bevanom* (the initial concentration, pH, volume of solution, and contact time was 50 mg L^{-1}, 7, 100 mL, and 90 min, respectively).

$$q_e = B \ln (K_T C_e) \quad (13)$$

where $B = (RT/A_T)$ and K_T is the Temkin constant.

The above equation is often readjusted as the linear form given below in order to simplify the calculation and plotting of Temkin constant. The B and K_T values can be calculated using the linear plot of q_e vs. ln (C_e) (Fig. 17).

$$q_e = B \ln K_T + B \ln C_e \quad (14)$$

The linearized form of the Temkin adsorption isotherm given in Eq. (14) was utilized to analyze the equilibrium data. The results are presented in Table 3.

3.7.4. The Dubinin–Radushkevich isotherm model

To determine the nature of the adsorption process viz. physisorption or chemisorption, the Dubinin–Radushkevick (D–R) [44–46] isotherm was employed. The following equation shows the linear form of this model:

$$\ln (q_e) = \ln (q_m) - \beta\varepsilon^2 \quad (15)$$

where q_e is the amount of Hg(II) adsorbed per unit dosage of the adsorbent (mg g^{-1}), q_m is the monolayer capacity, β is the activity coefficient related to the mean sorption energy and ε is the Polanyi potential given as:

$$\varepsilon = RT \ln \left(1 + \frac{1}{C_e}\right) \quad (16)$$

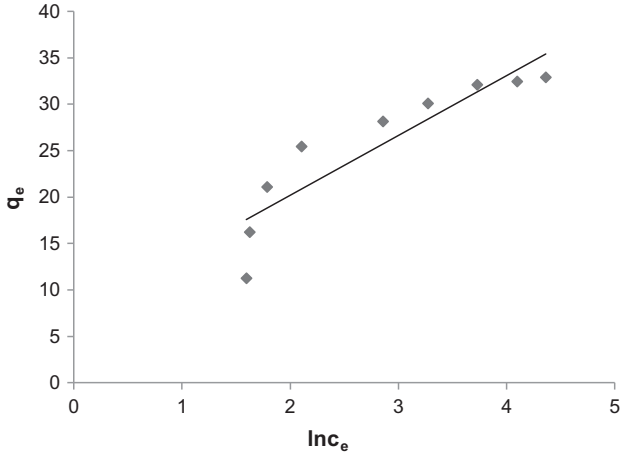

Fig. 17. Temkin sorption isotherm of mercury ions *onto S. bevanom* (the initial concentration, pH, volume of solution, and contact time was 50 mg L^{-1}, 7, 100 mL, and 90 min, respectively).

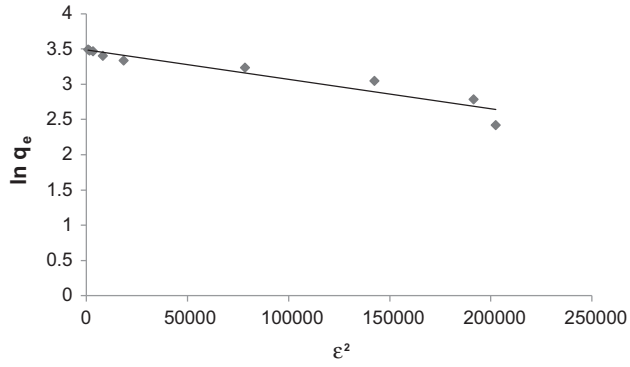

Fig. 18. Dubinin–Radushkevick sorption isotherm of mercury ions onto *S. bevanom* (the initial concentration, pH, volume of solution, and contact time was 50 mg L^{-1}, 7, 100 mL, and 90 min, respectively).

From the plots of ln q_e vs. ε^2 (Fig. 18), the values of β and q_m were obtained by the slope and intercept of the linear plot. Along with the isotherm constants, the statistical results are also given in Table 3. As can be seen from the results, the Hg(II) adsorption by *S. Bevanom* can be fitted with the Langmuir equation. Also, the D–R equation suggests that there is a considerable correlation factor. D–R isotherm shows that there is a close relationship between the heterogeneity of energies and the adsorbent surface. The quantity can be attributed to the mean sorption energy, E, which is the free energy for the transfer of 1 mol of metal ions from the infinity to the surface of the adsorbent [47]. One can calculate the mean free energy of the adsorption (E, kJ/mol) as follows [48]:

Table 4
The effect of temperature on the removal efficiency

Temperature (°C)	Removal efficiency of mercury (%)
20	90.12
35	91.45
50	93.65

Table 5
Thermodynamic parameter for adsorption of mercury onto *S. bevanom*

$\Delta H\left(\frac{kJ}{mol}\right)$	$\Delta S\left(\frac{kJ}{mol.K}\right)$	T (°C)	$\Delta G\left(\frac{kJ}{mol}\right)$	R^2
12.52	0.069	20	−5.3851	0.9783
		35	−6.06853	
		50	−7.22676	

Table 6
Comparison of the maximum sorption capacity (q_m) of the various sorbents

Sample	Sorbent material	q_m (mg g^{-1})	Refs.
1	*S. bevanom*	35.59	This work
2	Zeolite	1.21	[49]
3	Activated carbon	55.6	[50]
4	Polypyrrole-chitosan (PPy/CTN) nanocomposite	40	[51]
5	Rice husk ash	4	[52]
6	Chelating resin Chelex−100	14.19	[53]

$$E = (2\beta)^{-0.5} \quad (17)$$

It is said that the E magnitude is useful for the estimation of the adsorption type. If this value goes below 8 kJ/mol, the adsorption type can be explained by physical adsorption and a value between 8 and 16 kJ/mol indicates that the adsorption type can be explained by ion exchange. The E values found in this study were below 8 kJ/mol, suggesting that the mercury adsorption onto the *S. Bevanom* was considered as a physical adsorption [24].

3.8. Adsorption thermodynamics

3.8.1. Effect of temperature on adsorption of mercury

Experiments are performed at 20–50°C, pH 7, and materials value and adsorbent dosage level of 0.4 g in a 100 mL solution to study the effect of temperature adsorption. The equilibrium contact time for adsorption was maintained at 90 min. The increase in temperature from 20 to 50°C leads to a decrease in the percentage adsorption. The results are presented in Table 4. They revealed the exothermic nature of the adsorption process which was later used to determine the changes in Gibbs free energy (ΔG), heat of adsorption (ΔH), and entropy (ΔS) of the adsorption of NO_3^- from aqueous solutions.

3.8.2. Effect of temperature on thermodynamics parameter on adsorption of mercury

Thermodynamic constants such as enthalpy change ΔH, free energy change ΔG, and entropy change ΔS were calculated using Eqs. ((18)–(20)) to study the thermodynamics of Hg(II) adsorption on *S. Bevanom*. The values of these parameters are presented in Table 5. Using the following equations, the thermodynamic parameters, namely ΔH, ΔS, and ΔG, were calculated for Hg(II) on *S. Bevanom* system:

$$K_c = \frac{F_e}{1 - F_e} \quad (18)$$

$$\log K_c = \frac{-\Delta H}{2.303RT} + \frac{\Delta S}{2.303R} \quad (19)$$

$$\Delta G = -RT \ln K_c \quad (20)$$

where F_e is the fraction of Hg(II) ions sorbed at equilibrium. A study of Table 5 suggested that the enthalpy change, ΔH, is positive (endothermic) because of the increase in adsorption in successive increases in temperature. The negative ΔG values showed the thermodynamically feasible and spontaneous nature of the sorption. The positive value of ΔS indicates the increased randomness at the solid–solution interface during the ion fixation on the sorbent active sites.

3.9. Comparison of the maximum sorption capacity of various sorbents

To have a better understanding of the sorption capacity of *S. Bevanom*, the values of the maximum removal obtained for Hg(II) ion uptake with various types of sorbents are presented in Table 6. The experimental data collected from the present investigations are corresponding to the reported values. As seen in Table 6, the sorption capacity of *S. Bevanom* is higher than that of zeolite, Rice husk ash, and chelating resin Chelex-100.

4. Conclusion

Adsorption studies which were carried out on the *S. Bevanom* algae proved they are highly effective in the Hg(II) removal from aqueous solution. The conditions of sorption were as follows: a sorbent dose of 0.4 g in a 100 mL solution. The optimum contact time and pH were 90 min and 7, respectively. The kinetic data showed that the adsorption process was governed by Morris–Weber model. The results of this study were well explained by the theoretical Langmuir. Thermodynamic studies showed a negative

ΔG and positive ΔS and ΔH. Results were indicative of the endothermic nature of the adsorption. The negative ΔG values showed the thermodynamically feasible and spontaneous nature of the sorption. The positive value of ΔS demonstrates the increased randomness at the solid–solution interface during the ion fixation on the sorbent sites. An analysis of the relationship between the predicted results of the designed ANN model and the experimental data showed that the Hg (II) adsorption was given by the *S. Bevanom* algae and predicted by the application of a 3-layered neural network having 6 neurons in the hidden layer. In conclusion, an ANN model-based simulation can provide further contribution to develop a better understanding of the dynamic behavior of the process in which there are still some unfathomable phenomena that cannot be explained with all details.

References

[1] J. Dong, Z. Xu, F. Wang, Engineering and characterization of mesoporous silica-coated magnetic particles for mercury removal from industrial effluents, Appl. Surf. Sci. 254 (2008) 3522–3530.

[2] R. Katal, M. Ghiass, H. Esfandian, Application of nanometer size of polypyrrole as a suitable adsorbent for removal of Cr(VI), J. Vinyl Add. Technol. 17 (2011) 222–230.

[3] M. Morita, J. Yoshinaga, J.S. Edmonds, The determination of mercury species in environment and biological samples, Pure. Appl. Chem. 70 (1998) 1585–1615.

[4] P.J. Cyr, P.S. Suri, E.D. Helmig, A pilot scale evaluation of removal of mercury from pharmaceutical wastewater using granular activated carbon, Water Res. 36 (2002) 4725–4734.

[5] F. Berglund, M. Bertin, Chemical Fallout, Thomas Publishers, Spring field, 1969.

[6] C.R. Krishnamoorthi, P. Vishwanathan, Toxic Metal in the Indian Environment, Tata Mc Graw Hill Publishing Co. Ltd, New Delhi, (1991) 188–198.

[7] Z. He, S. Siripornadulsil, R.T. Sayre, S.J. Traina, L.K. Weavers, Removal of mercury from sediment by ultrasound combined with biomass (transgenic *Chlamydomonas reinhardtii*), Chemosphere 83 (2011) 1249–1254.

[8] Q. Wan, L. Duan, K. He, J. Li, Removal of gaseous elemental mercury over a CeO_2–WO_3/TiO_2 nanocomposite in simulated coal-fired flue gas, Chem. Eng. J. 170 (2011) 512–517.

[9] V.K. Verma, S. Tewari, J.P.N. Rai, Ion exchange during heavy metal bio-sorption from aqueous solution by dried biomass of macrophytes, Bioresour. Technol. 99 (2008) 1932–1938.

[10] A. Ahmadpour, M. Tahmasbi, T. Bastami Rohani, J.A. Besharati, Rapid removal of cobalt ion from aqueous solutions by almond green hull, J. Hazard. Mater. 166 (2009) 925–930.

[11] H.S. Abbas, E.E. Shahlaa, M.A. Sama, J.A.M. Tariq, Removal of lead, cadmium, and mercury ions using biosorption, Desalin. Water Treat. 24 (2010) 344–352.

[12] S. Kumar, B.C. Meikap, Removal of Chromium(VI) from waste water by using adsorbent prepared from green coconut shell, Desalin. Water Treat. 52 (2014) 3122–3132.

[13] R. Katal, M. Sharifzadeh Baei, H.T. Rahmati, H. Esfandian, Kinetic, isotherm and thermodynamic study of nitrate adsorption from aqueous solution using modified rice husk, J. Ind. Eng. Chem. 18 (2012) 295–302.

[14] S. Hussain, S. Gul, S. Khan, H. Rehman, M. Ishaq, A. Khan, F. Akbar Jan, Z.U. Din, Removal of Cr(VI) from aqueous solution using brick kiln chimney waste as adsorbent, Desalin. Water Treat. 53 (2013) 1–9.

[15] N. Milosavljević, A. Debeljković, M. Kalagasidis Krušić, N. Milašinović, Ö.B. Üzüm, E. Karadağ, Application of poly(acrlymide-co-sodium methacrylate) hydrogels in copper and cadmium removal from aqueous solution, Environ. Prog. Sustainable Energy 33 (2014) 824–834.

[16] P. Lodeiro, R. Herrero, M.E. Sastre de Vicente, The use of protonated *Sargassum muticum* as biosorbent for cadmium removal in a fixed-bed column, J. Hazard. Mater. 137 (2006) 244–253.

[17] S. Ahmad, I.H. Qureshi, Fast mecury removal from industrial effluent, J. Radioanal. Nucl. Chem. Art. 130 (1989) 347–352.

[18] B. Shyamala Devi, S. John Mary, S. Rajendran, N. Manimaran, P. Rengan, J. Jayasundari, M. Mannivannan, Removal of mercury by biosorption onto *Sphaeroplea* algae, ZAŠTITA MATERIJALA. 51 (2010) 227–231.

[19] R. Jayakumar, M. Rajasimman, C. Karthikeyan, Sorption of hexavalent chromium from aqueous solution using marine green algae *Halimeda gracilis* : Optimization, equilibrium, kinetic, thermodynamic and desorption studies, J. Environ. Chem. Eng. 2 (2014) 1261–1274.

[20] S.M. Hosseini Asl, M. Ahmadi, M. Ghiasvand, A. Tardast, R. Katal, Artificial neural network (ANN) approach for modeling of Cr(VI) adsorption from aqueous solution by zeolite prepared from raw fly ash (ZFA), J. Ind. Eng. Chem. 19 (2013) 1044–1055.

[21] M. Fagundes-Klen, P. Ferri, T. Martins, C. Tavares, E. Silva, Equilibrium study of the binary mixture of cadmium–zinc ions biosorption by the *Sargassum filipendula* species using adsorption isotherms models and neural network, Biochem. Eng. J. 34 (2007) 136–146.

[22] N.G. Turan, B. Mesci, O. Ozgonenel, The use of artificial neural networks (ANN) for modeling of adsorption of Cu(II) from industrial leachate by pumice, Chem. Eng. J. 171 (2011) 1091–1097.

[23] H. Esfandian, H.R. Javadian, M. Parvini, B. Khoshandam, Batch and column removal of copper by modified brown algae *Sargassum bevanom* from aqueous solution, Asia. Pac. J. Chem. Eng. 8 (2013) 665–678.

[24] H. Javadian, M. Ahmadi, M. Ghiasvand, S. Kahrizi, R. Katal, Removal of Cr(VI) by modified brown algae *Sargassum bevanom* from aqueous solution and industrial wastewater, J. Taiwan. Inst. Chem. Eng. 44 (2013) 977–989.

[25] V.K. Gupta, A. Rastogi, Biosorption of hexavalent chromium by raw and acid-treated green alga *Oedogonium hatei* from aqueous solutions. J. Hazard. Mater. 163 (2009) 396–402.

[26] K. Vijayaraghavan, J. Jegan, K. Palanivelu, M. Velan, Batch and column removal of copper from aqueous solution using a brown marine alga *Turbinaria ornata*, Chem. Eng. J. 106 (2005) 177–184.
[27] Standard Methods for the Examination of Water and Wastewater, American Public Health Association/ AmericanWater Works Association/Water Environment Federation, Washington, DC, (1989).
[28] I. Chairez, I. García-Peña, A. Cabrera, Dynamic numerical reconstruction of a fungal biofiltration system using differential neural network, J. Process Control 19 (2009) 1103–1110.
[29] E.R. Rene, M.C. Veiga, C. Kennes, Experimental and neural model analysis of styrene removal from polluted air in a biofilter, J. Chem. Technol. Biotechnol. 84 (2009) 941–948.
[30] A. Elías, G. Ibarra-Berastegi, R. Arias, A. Barona, Neural networks as a tool for control and management of a biological reactor for treating hydrogen sulphide, Bioprocess. Biosyst. Eng. 29 (2006) 129–136.
[31] H.R. Maier, G.C. Dandy, Neural networks for the prediction and forecasting of water resources variables: A review of modelling issues and applications, Environ. Modell. Software 15 (2000) 101–124.
[32] K. Movagharnejad, M. Nikzad, Modeling of tomato drying using artificial neural network, Comput. Electron. Agric. 59 (2007) 78–85.
[33] R.M. Aghav, S. Kumar, S.N. Mukherjee, Artificial neural network modeling in competitive adsorption of phenol and resorcinol from water environment using some carbonaceous adsorbents, J. Hazard. Mater. 188 (2011) 67–77.
[34] D. Park, Y.S. Yun, J.M. Park, Reduction of hexavalent chromium with the brown seaweed *Ecklonia* biomass, Environ. Sci. Technol. 38 (2004) 4860–4864.
[35] R. Katal, E. Hasani, M. Farnam, M. Sharifzadeh Baei, M.A. Ghayyem, Charcoal ash as an adsorbent for Ni (II) adsorption and its application for wastewater treatment, J. Chem. Eng. Data 57 (2012) 374–383.
[36] W.J. Weber, J.C. Morris, Kinetics of adsorption on carbon from solution, J. Sanit. Eng. Div. 89 (1963) 31–59.
[37] A.K. Bhattacharya, T.K. Naiya, S.N. Mandal, S.K. Das, Adsorption, kinetics and equilibrium studies on removal of Cr(VI) from aqueous solutions using different low-cost adsorbents, Chem. Eng. J. 137 (2008) 529–541.
[38] M. Vafaie Sefti, M. Jafari, A.M. Saeedi, M. Sharifian, R. Katal, Study effect of different parameter on the sulfate sorption onto nanoalumina, J. Ind. Eng. Chem. 18(1) (2012) 230–236.
[39] G. Limousin, J.-P. Gaudet, L. Charlet, S. Szenknect, V. Barthès, M. Krimissa, Sorption isotherms: A review on physical bases, modeling and measurement, Appl. Geochem. 22 (2007) 249–275.
[40] I. Langmuir, The adsorption of gases on plane surfaces of glass, mica and platinum, J. Am. Chem. Soc. 40 (1918) 1361–1403.
[41] H. Esfandian, M. Jafari, M. Alizadeh, H.T. Rahmati, R. Katal, Synthesis of polyaniline nanocomposite and its application for chromium removal from aqueous solution, J. Vinyl. Add. Technol. 18 (2012) 250–260.
[42] H. Freundlich, Of the adsorption of gases. Section II. Kinetics and energetics of gas adsorption. Introductory paper to section II, Trans. Faraday Soc.28 (1932) 195– 201.
[43] M.J. Temkin, V. Pyzhev, Recent modifications to Langmuir isotherms, Acta Physiochim , URSS. 12 (1940) 217–222.
[44] M.M. Dubinin, L.V. Radushkevich, Equation of the characteristic curve of activated charcoal, Chem. Zentr. 1 (1947) 875–889.
[45] T.S. Anirudhan, P.S. Suchithra, Humic acid-immobilized polymer/bentonite composite as an adsorbent for the removal of copper(II) ions from aqueous solutions and electroplating industry wastewater, J. Ind. Eng. Chem. 16 (2010) 130–139.
[46] S.E. Ghazy, A.H. Ragab, Removal of copper from water samples by sorption onto powdered limestone, Ind. J. Chem. Technol. 14 (2007) 507–514.
[47] T.K. Naiya, A.K. Bhattacharya, S.K. Das, Removal of Cd(II) from aqueous solutions using clarified sludge, J. Colloid Interface Sci. 325 (2008) 48–56.
[48] W.S. Wan, S. Ngah, Fatinathan, Adsorption characterization of Pb(II) and Cu(II) ions onto chitosan-tripolyphosphate beads: Kinetic, equilibrium and thermodynamic studies, J. Environ. Manage. 91 (2010) 958–969.
[49] A. Chojnacki, K. Chojnacka, J. Hoffmann, H. Górecki, The application of natural zeolites for mercury removal: From laboratory tests to industrial scale, Miner. Eng. 17 (2004) 933–937.
[50] K. Kadirvelu, M. Kavipriya, C. Karthika, N. Vennilamani, S. Pattabhi, Mercury(II) adsorption by activated carbon made from sago waste, Carbon. 42 (2004) 745–752.
[51] S. Salahi, M. Ghorban, Adsorption parameters studies for the removal of mercury from aqueous solutions using hybrid sorbent, Adv. Polym. Technol. 33 (2014) 1–6.
[52] A.G. El-Said, N.A. Badawy, S.E. Garamon, Adsorption of cadmium(II) and mercury(II) onto natural adsorbent rice husk ash (RHA) from aqueous solutions: Study in single and binary system, J. Am. Sci. 6(12) (2010) 400–409.
[53] A. Amara-Rekkab, M.A. Didi, Liquid—solid extraction of hg(ii) from aqueous solution by chelating resin chelex-100, Eur. Chem. Bull. 3(9) (2014) 860–868.